

The effect of the geometric phase on spin-polarized electron tunnelling

This article has been downloaded from IOPscience. Please scroll down to see the full text article.

2004 J. Phys.: Condens. Matter 16 6713

(<http://iopscience.iop.org/0953-8984/16/37/007>)

View [the table of contents for this issue](#), or go to the [journal homepage](#) for more

Download details:

IP Address: 129.252.86.83

The article was downloaded on 27/05/2010 at 17:32

Please note that [terms and conditions apply](#).

The effect of the geometric phase on spin-polarized electron tunnelling

Zheng-Chuan Wang¹, Gang Su¹, Ling Li² and Jie Gao²

¹ Department of Physics, The Graduate School of the Chinese Academy of Sciences,
PO Box 3908, Beijing 100039, People's Republic of China

² Department of Physics, Sichuan University, Chengdu 610018, People's Republic of China

Received 15 April 2004, in final form 20 July 2004

Published 3 September 2004

Online at stacks.iop.org/JPhysCM/16/6713

doi:10.1088/0953-8984/16/37/007

Abstract

In order to explore the effect of the geometric phase on the spin-polarized electron tunnelling in a ferromagnet/insulator/ferromagnet (FM/I/FM) junction, in this paper, we apply a voltage drop in the insulating layer and allow it to vary adiabatically with time t . Then the wavefunction will acquire a geometric phase which will give rise to an observable effect on the physical quantities of interest. The numerical results indicate that the geometric phase certainly has an influence on the differential conductance and the tunnelling magnetoresistance (TMR) in the spin-polarized tunnelling. We also show results for the conductance and TMR obtained by changing the orientation angle and the magnitude of the molecular field in the ferromagnets. An experimental profile for observing the effect of the geometric phase on the spin-polarized electron transport in a FM/I/FM tunnel junction is suggested.

1. Introduction

Spin-polarized electron tunnelling, since its realization 30 years ago, has been widely explored both experimentally and theoretically. In particular, the tunnelling through a ferromagnet/insulator/ferromagnet (FM/I/FM) junction has attracted much more attention [1–4]. In 1989, Slonczewski [5] proposed a free electron model for analytically studying the transmission of charge and spin currents flowing through a tunnelling junction. Following this model, Zhang *et al* [6, 7] further studied the tunnelling through ferromagnet/insulator (semiconductor) single and double junctions subject to a dc bias. However, studies of the theory of time dependent transport through this tunnelling junction are, as far as we are aware, still rare. We are aware of some papers in the recent past which treat time dependent phenomena using non-equilibrium Green function (NEGF) theory in mesoscopic physics [8]. A few years ago, Büttiker and co-workers [9–11] proposed, in the framework of the scattering matrix approach, an ac transport theory to explain the differential conductance and electrochemical capacitance in mesoscopic systems. Wang *et al* [12] further employed this theory to explore the

ac transport properties in the spin-polarized tunnelling of the FM/I(S)/FM junction. However, this method, based on the scattering matrix or the NEGF theory, always involves performing some complicated numerical calculations, so it is worthwhile to develop an explicit time dependent transport theory and to deal analytically with the spin-polarized tunnelling problem.

The time dependent transport problem can be studied analytically in some special cases—for instance, when the voltage drop varies adiabatically with time t . As is known, if the quantum system varies adiabatically, which means that the external probe is slowly turned on, in accordance with the adiabatic theorem [13], the wavefunction will acquire a geometric phase [14] in addition to the familiar dynamical phase $\exp(-iEt/\hbar)$. The effect is also predicted to occur for spin-polarized tunnelling. In fact, the geometric phase has played an important role in mesoscopic transport problems. In the past, geometric phases were widely used to study quantum Hall effects [15] as well as adiabatic quantum electron pumping [16]. Brouwer [17] presented a formula for studying the pumped current based on the theory of the emissivities of the system proposed by Büttiker *et al* [18]. Avron [19] further related the charge in the adiabatic mesoscopic quantum pump to Berry's phase and the corresponding Brouwer pumping formula to the curvature. An experiment used interference to directly measure the geometric phase of scattering states in nanoscale electric devices in a manner similar to that used to observe quantum adiabatic charge pumping by Zhou *et al* [20]. It is the purpose of this paper to investigate the influence of the geometric phase on the spin-polarized tunnelling transport in the FM/I/FM junction. Our approach is similar to Slonczewski's, but the wavefunction is associated with the geometric phase induced by the adiabatic procedure. The differential conductance associated with the geometric phase can be obtained by matching the wavefunctions in different regions via the continuity conditions and their derivatives.

The rest of this paper can be outlined as follows. The formalism of the adiabatic quantum transport for a spin-polarized tunnelling junction will be described in section 2. In section 3, we shall present our numerical analyses of the differential conductance as well as the tunnelling magnetoresistance (TMR) under the influence of the geometric phase. Finally, a brief summary is given in section 4, and the complicated equations for the matching coefficients are given in the appendix.

2. The general formalism

Consider a FM/I/FM tunnelling junction which is connected by two electron reservoirs at contacts $\alpha = 1, 2$. For convenience, we neglect the difference in electron effective mass of the barrier and ferromagnets, and treat both masses as the bare electron mass m . The system consists of left and right ferromagnet layers with semi-infinite width, and an insulating layer with a thickness d which is between the two ferromagnet layers. The magnitudes of the molecular fields associated with the left and right ferromagnet layers are assumed to be h_1 and h_2 , and the barrier height in the insulator is supposed to be U . To see the effect of the geometric phase on the spin-polarized tunnelling transport, a voltage drop $V(x, t)$, which varies with position x and adiabatically with time t , is applied in the insulator layer. In fact, this voltage drop is just a special case of a two-parameter pumping. This kind of pumping had been discussed clearly in the paper of Usmani *et al* [21] for the classical case. In their paper, the pumping can be chosen as the perturbation: $\Delta V(x, T(t)) = -V_A \cos(2\pi x/a) \cos(\omega t) - V_B \cos(2\pi x/a + \chi) \cos(\omega t + \varphi)$, which is similar to the potential adopted in our system, where we chose $V_A = -V_0$, $V_B = V_0$ and $\chi = \varphi = \pi/2$. Certainly, this voltage drop must be adiabatically turned on in order to preserve the adiabatic transport in the FM/I(S)/FM tunnelling junction. Then the wavefunction in the insulator will

acquire a geometric phase $\gamma(x, t)$ during this adiabatic procedure:

$$\Psi(x, t) = \exp(-iEt/\hbar) \exp(i\gamma(x, t))u_E(x, t), \quad (1)$$

where the geometric phase $\gamma(x, t)$ takes a form as in [14]:

$$\gamma(x, t) = i \int_0^t \langle u_E(x, t') | \frac{\partial}{\partial t'} | u_E(x, t') \rangle dt'. \quad (2)$$

The eigenfunction $u_E(x, t)$ obeys the following eigenequation:

$$Hu_E(x, t) = Eu_E(x, t), \quad (3)$$

where H is the Hamiltonian of the system. In the FM/I/FM tunnelling junction,

$$H = -\frac{\hbar^2}{2m} \frac{d^2}{dx^2} + U(x) + \mathbf{h}(\mathbf{x}) \cdot \boldsymbol{\sigma} + \mathbf{V}(\mathbf{x}, t),$$

with

$$U(x) + \mathbf{h}(\mathbf{x}) \cdot \boldsymbol{\sigma} + \mathbf{V}(\mathbf{x}, t) = \begin{cases} \mathbf{h}_1 \cdot \boldsymbol{\sigma}, & x \leq 0, \\ U + V(x, t), & 0 < x < d, \\ \mathbf{h}_2 \cdot \boldsymbol{\sigma}, & x \geq d, \end{cases}$$

where \mathbf{h}_1 and \mathbf{h}_2 are the molecular fields in the left and right ferromagnets, $\boldsymbol{\sigma}$ is the Pauli matrix, U is the barrier height in the insulator, $V(x, t)$ is the voltage drop applied in the insulator layer.

To proceed further, a semiclassical WKB approximation (up to first order) may be adopted; then the eigenfunction $u_E(x, t)$ in the insulator barrier with a voltage drop $V(x, t)$ can be analytically written as

$$u_E(x, t) = R(x, t) \exp(iS(x, t)/\hbar), \quad (4)$$

with

$$R(x, t) = [2m(E - U - V(x, t))]^{-\frac{1}{4}} \quad (5)$$

and

$$S(x, t) = \int^x \sqrt{2m(E - U - V(x', t))} dx'. \quad (6)$$

The above formulae hold only under the WKB approximation condition $|\frac{d\lambda}{dx}| \ll 1$, where $\lambda = \frac{\hbar}{\sqrt{2m(E - U - V(x, t))}}$. Taking them together with equations (4)–(6), the geometric phase can be further expressed as

$$\gamma(x, t) = i \int_0^t \left[R(x, t') \frac{\partial}{\partial t'} R(x, t') + \frac{i}{\hbar} R^2(x, t') \frac{\partial}{\partial t'} S(x, t') \right] dt'. \quad (7)$$

This expression implies that the geometric phase is mainly dominated by the adiabatic time variation of the voltage drop $V(x, t)$.

Now we begin to write down the wavefunctions in the ferromagnets and insulator. Let us consider a spin up incident wave with unit incident flux. Then, the wavefunction in the left contact of the ferromagnet can be chosen as

$$\Psi_{1\uparrow} = \exp(ik_{1\uparrow}x) + R_{\uparrow} \exp(-ik_{1\uparrow}x) \quad (8)$$

and

$$\Psi_{1\downarrow} = R_{\downarrow} \exp(-ik_{1\downarrow}x), \quad (9)$$

where $hk_{1\uparrow,\downarrow} = \sqrt{2m(E \mp \hbar_1)}$. In the insulator, we should consider the influence of the geometric phase induced by the adiabatic variation of the voltage drop $V(x, t)$ with time t , and the wavefunction must adopt the form of (1), namely

$$\begin{aligned} \Psi_{2\uparrow} &= A_{\uparrow} \exp(i\gamma^+(x, t)) [2m(E - U - V(x, t))]^{-\frac{1}{4}} \\ &\quad \times \exp\left(\frac{i}{\hbar} \int^x \sqrt{2m(E - U - V(x', t))} dx'\right) \\ &\quad + B_{\uparrow} \exp(i\gamma^-(x, t)) [2m(E - U - V(x, t))]^{-\frac{1}{4}} \\ &\quad \times \exp\left(-\frac{i}{\hbar} \int^x \sqrt{2m(E - U - V(x', t))} dx'\right) \end{aligned} \quad (10)$$

and

$$\begin{aligned} \Psi_{2\downarrow} &= A_{\downarrow} \exp(i\gamma^+(x, t)) [2m(E - U - V(x, t))]^{-\frac{1}{4}} \\ &\quad \times \exp\left(\frac{i}{\hbar} \int^x \sqrt{2m(E - U - V(x', t))} dx'\right) \\ &\quad + B_{\downarrow} \exp(i\gamma^-(x, t)) [2m(E - U - V(x, t))]^{-\frac{1}{4}} \\ &\quad \times \exp\left(-\frac{i}{\hbar} \int^x \sqrt{2m(E - U - V(x', t))} dx'\right), \end{aligned} \quad (11)$$

where $A_{\uparrow,\downarrow}$ and $B_{\uparrow,\downarrow}$ are coefficients related to the incident wave and the reflected wave, respectively. The geometric phase $\gamma^+(x, t)$ corresponding to the incident wave from left to right is

$$\gamma^+(x, t) = i \int_0^t \left[R(x, t') \frac{\partial}{\partial t'} R(x, t') + \frac{i}{\hbar} R^2(x, t') \frac{\partial}{\partial t'} S(x, t') \right] dt', \quad (12)$$

and the geometric phase $\gamma^-(x, t)$ related to the reflected wave in the insulator is

$$\gamma^-(x, t) = i \int_0^t \left[R(x, t') \frac{\partial}{\partial t'} R(x, t') - \frac{i}{\hbar} R^2(x, t') \frac{\partial}{\partial t'} S(x, t') \right] dt'. \quad (13)$$

The wavefunction in the right ferromagnet just contains the transmitted wave

$$\Psi_{3\uparrow} = C_{\uparrow} \exp(ik_{3\uparrow}x) \quad (14)$$

and

$$\Psi_{3\downarrow} = C_{\downarrow} \exp(ik_{3\downarrow}x), \quad (15)$$

where $hk_{3\uparrow,\downarrow} = \sqrt{2m(E \mp \hbar_2)}$. Both the wavefunctions $\Psi_{1\uparrow,\downarrow}$ and $\Psi_{3\uparrow,\downarrow}$ are for the independent electrons, and $\Psi_{2\uparrow,\downarrow}$ includes the effect of the geometric phase.

To complete the above wavefunction, we must find the unknown coefficients $R_{\uparrow,\downarrow}$, $A_{\uparrow,\downarrow}$, $B_{\uparrow,\downarrow}$ and $C_{\uparrow,\downarrow}$ by matching the wavefunctions and their derivatives at the interfaces $x = 0$ and L . The wavefunctions require the following spinor transformation at $x = 0$:

$$\begin{pmatrix} \Psi_{1\uparrow}(x) \\ \Psi_{1\downarrow}(x) \end{pmatrix} = \begin{pmatrix} \cos \theta_1 & \sin \theta_1 \\ -\sin \theta_1 & \cos \theta_1 \end{pmatrix} \begin{pmatrix} \Psi_{2\uparrow}(x) \\ \Psi_{2\downarrow}(x) \end{pmatrix} \quad (16)$$

and similarly for the derivatives at $x = 0$, where θ_1 is the angle between the molecular field \mathbf{h}_1 and the z axis. In the same manner, we can write down similar expressions for the wavefunction and their derivatives at the interface $x = L$:

$$\begin{pmatrix} \Psi_{2\uparrow}(x) \\ \Psi_{2\downarrow}(x) \end{pmatrix} = \begin{pmatrix} \cos \theta_2 & \sin \theta_2 \\ -\sin \theta_2 & \cos \theta_2 \end{pmatrix} \begin{pmatrix} \Psi_{3\uparrow}(x) \\ \Psi_{3\downarrow}(x) \end{pmatrix}.$$

Armed with the above wavefunctions $\Psi_{1\uparrow,\downarrow}$, $\Psi_{2\uparrow,\downarrow}$ and $\Psi_{3\uparrow,\downarrow}$, we can write down the matching conditions in terms of the spinor transformation condition at the interface $x = 0$

and L . They are eight linear equations in the unknown coefficients $R_{\uparrow,\downarrow}$, $A_{\uparrow,\downarrow}$, $B_{\uparrow,\downarrow}$ and $C_{\uparrow,\downarrow}$. After some algebraic calculations, we can obtain analytically the coefficients appearing in the wavefunctions. We collect these expressions for C_{\uparrow} and C_{\downarrow} in the appendix; they will be used later to express the differential conductance, from which we can see the influence of the geometric phase.

We proceed to study the differential conductance and the tunnelling magnetoresistance (TMR) with the above-obtained analytical wavefunctions. It is well known that the probability flux density in quantum mechanics is

$$f = \frac{1}{2m} \left(\Psi^* \frac{\hbar}{i} \nabla \Psi + \text{c.c.} \right). \quad (17)$$

From the above analytical expression for the wavefunction, we can express this flux analytically. Then, along with some statistical considerations, the differential conductance can be obtained analytically. For that purpose, we first express the transmission coefficient as

$$T(E) = \sum_{s,s'} T_{s,s'}, \quad (18)$$

where $s, s' = \uparrow, \downarrow$ and

$$T_{s,s'} = \frac{f_{\text{tran},s'}}{f_{\text{inc},s}} = \frac{k_{3s'}}{k_{1s}} |C_{s'}|^2, \quad (19)$$

where $f_{\text{tran},s'} = \frac{\hbar k_{3s'}}{m} |C_{s'}|^2$ is the transmitted probability flux density and $f_{\text{inc},s} = \frac{\hbar k_{1s}}{m}$ is the incident probability flux density. In a two-terminal measurement, the voltage and current are measured through the same set of leads. For the single-channel case in a 1D system, the conductance follows the Landauer formula [22]:

$$\begin{aligned} G(t) &= \left(\frac{e^2}{h} \right) T \\ &= \left(\frac{e^2}{h} \right) \sum_{s'} \frac{k_{3s'}}{k_{1\uparrow}} |C_{s'}|^2. \end{aligned} \quad (20)$$

Since we only consider the spin up incident electron in our case, the sum in equation (20) does not include the s index. The coefficients $C_{s'}$ ($s' = \uparrow, \downarrow$) satisfying the boundary conditions at the interface $x = L$ are given in the appendix. Equation (20) now represents the conductance in the presence of the geometric phase, which depends on time t . The time-averaged conductance in one adiabatic cycle T of the voltage drop in the insulator can be defined as

$$G = \frac{1}{T} \int_0^T G(t') dt'. \quad (21)$$

It is sufficient to average over the period because the voltage drop $V(x, t)$ can be a periodic function of time.

We next consider the tunnelling magnetoresistance which is defined as

$$\text{TMR} = \frac{G_0 - G_\pi}{G_0}, \quad (22)$$

where G_π and G_0 are the conductance corresponding to the orientation angle θ_2 of the molecular field, taken as π and 0, respectively, and $\theta_1 = 0$; they have been averaged over t . With the analytical expression for the differential conductance, we can demonstrate the influence of the geometric phase on the TMR analytically.

When we vary the voltage drop with time t adiabatically, the differential conductance and TMR will differ from the corresponding physical quantities in the case of a time independent

voltage drop, because the geometric phase originating from the adiabatic procedure will have an effect on the differential conductance and TMR, so in mesoscopic transport theory, one should consider the influence of the geometric phase, which will help us to obtain the correct theoretical results. If we set the geometric phases $\gamma^+(x, t)$ and $\gamma^-(x, t)$ appearing in the above expressions to zero, which means dropping out the geometric phase, the conductance and TMR are, obviously, different from the results obtained for the geometric phase. We may see their difference directly in the analytical expressions. However, such a comparison just embodies the difference in theoretical treatment; how to observe the influence of the geometric phase experimentally is an interesting question, which we now try to address.

In fact, the geometric phase has an effect only via the probability flux density (17), thereby leading to its influence on the differential conductance and TMR. Substituting the wavefunction (1) including the geometric phase into the expression for the probability flux density, we have

$$f(x, t) = \frac{1}{2m} \left\{ \left[\exp(iEt/\hbar) \exp(-i\gamma(x, t)) u_E^*(x, t) \frac{\hbar}{i} (\exp(-iEt/\hbar) \exp(i\gamma(x, t)) \nabla u_E(x, t) + \exp(-iEt/\hbar) i \nabla \gamma(x, t) \exp(i\gamma(x, t)) u_E(x, t)) \right] + \text{c.c.} \right\}. \quad (23)$$

The influence of the geometric phase comes from the second term and its conjugate. From expression (7) for the geometric phase and equations (5) and (6), we see that the geometric phase changes with x ; thus its gradient is non-zero only when the voltage drop in the insulator layer varies with the space coordinate x . If the voltage drop in the insulator does not depend on the coordinate x , the second term and its conjugate in (23) will vanish, and then the geometric phase will not give rise to any observable effect on the differential conductance and TMR. However, if we impose a voltage drop $V(x, t)$ which not only depends on the coordinate x but also varies adiabatically with t in the insulator of a FM/I/FM junction, we could observe the change of the differential conductance and TMR induced by the geometric phase by comparing the results obtained with the case in which the voltage drop takes a similar functional form but is independent of x , say, $V(t)$. In this way, one may experimentally examine the effect of the geometric phase on an observably physical quantity. This is also an alternative way to verify the existence of the geometric phase in a real physical system.

3. Numerical analysis

In our numerical calculations we shall take the width of the insulator layer to be 5.0 nm. For the sake of simplicity, the magnitudes of the molecular fields in the FM layers are both assumed to be 0.2 eV, and the barrier height U in the insulator is supposed to be 0.3 eV. The effective mass is taken as the same for the ferromagnet and insulator. The voltage drop in the insulator layer adopts the form of a cosine function $V(x, t) = V_0 \cos(kx - \omega t)$, where the variation with time is adiabatic. The criterion of adiabaticity in this case is that the electron system has time to adjust to the varying voltage drop; V_0 is the amplitude of the voltage drop, k is the wavevector and ω is the frequency. This voltage drop must be adiabatically turned on. We have plotted them in figures 1(a) and (b) at different times and different amplitudes V_0 .

The results for the differential conductance G involving the geometric phase as a function of the amplitude V_0 of the voltage drop are presented in figure 2, where the angle θ_1 of the molecular field in the left ferromagnet is chosen as 0 and the angle θ_2 in the right ferromagnet is $\pi/6$. For comparison, we also plot the curve of the differential conductance G_0 versus V_0 , for which the geometric phase is missing (chosen simply as zero). It can be seen that the geometric phase induced by the adiabatic variation of time t in the voltage drop $V(x, t)$ has

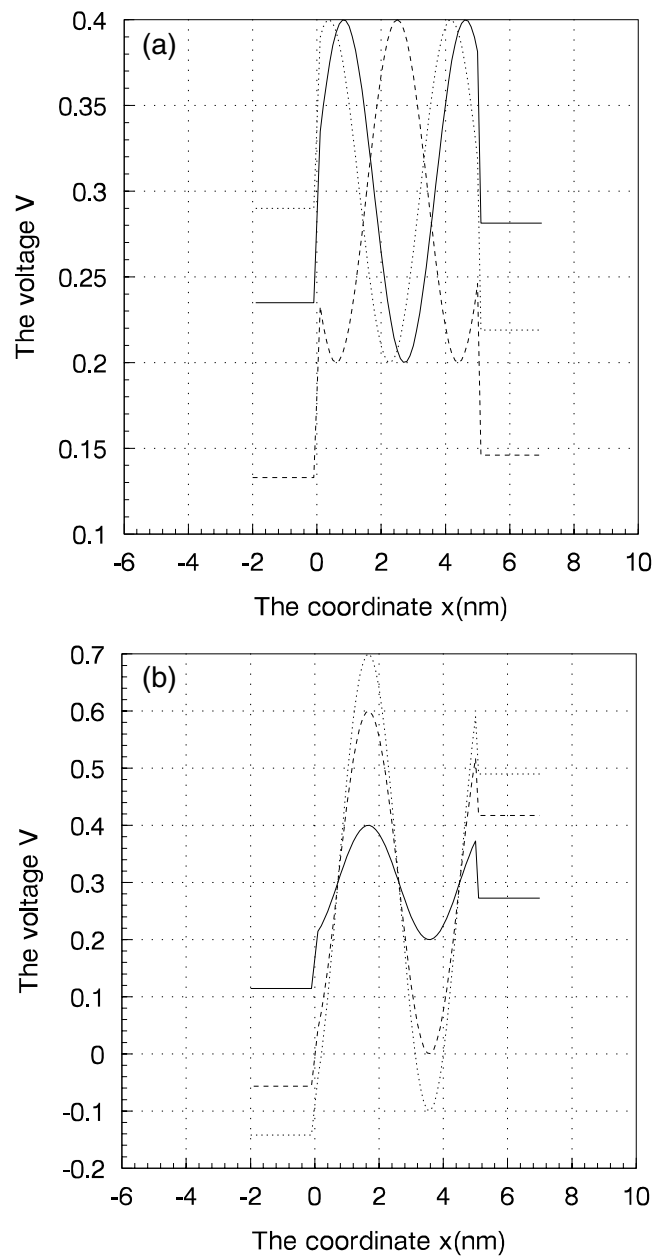


Figure 1. (a) The voltage drop in all regions of the structure at different times, where the amplitude V_0 is taken as 0.1 eV and the length of the insulator is 5 nm. The full curve corresponds to $\omega t = \pi/3$, while for the dashed curve and the dotted curve, ωt is taken as π and $5\pi/3$, respectively. (b) The voltage drop in all regions of the structure at different amplitudes V_0 where ωt is taken as $\pi/3$. The full line corresponds to $V_0 = 0.1$ eV, while for the dashed curve and the dotted curve, V_0 is taken as 0.3 and 0.5 eV, respectively.

obvious effects on the differential conductance G . The conductance G_0 varies slowly with V_0 below 0.20 eV, but increases rapidly above 0.20 eV; however, the conductance G has a big dip

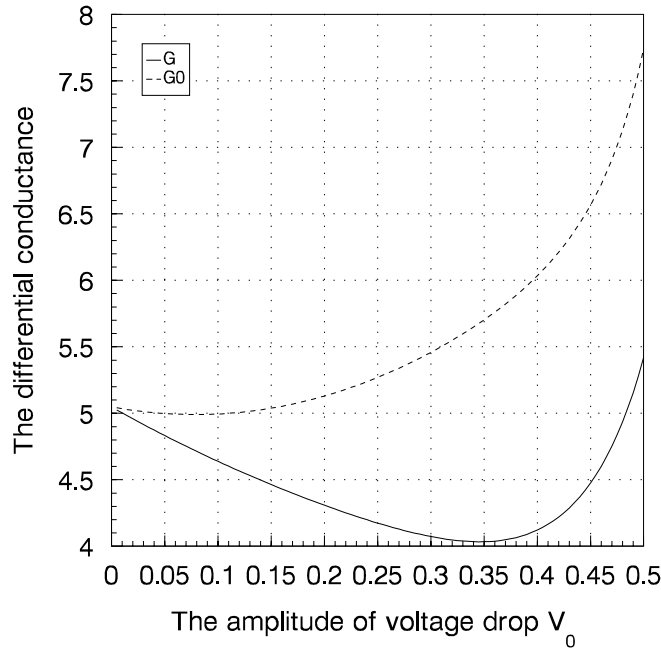


Figure 2. The conductance G (unit e^2/h) associated with the geometric phase and the conductance $G0$ at which the geometric phase is dropped out versus the amplitude of the voltage drop V_0 , where the length of the insulator is 5 nm, the angles θ_1 and θ_2 of the molecular fields in the left and right ferromagnets are 0 and $\pi/6$, respectively, and the magnitudes of the molecular fields in the left and right ferromagnets are both 0.3 eV. The dashed curve shows the conductance $G0$ and the solid curve shows the conductance G .

at 0.35 eV, whose value is always smaller than $G0$, which is due to the interference effect of the geometric phase. When we include the geometric phase in the wavefunction, the incident wave and the reflected wave in the insulator bear different geometric phases; they will interfere with each other, as characterized by the interference term in the expression for $C_{\uparrow,\downarrow}$. It is this property that makes the value of the differential conductance smaller.

When we change the angle θ_2 of the molecular field in the right ferromagnet from $\pi/6$ to $\pi/4$, the curve of the differential conductance G concerned with the geometric phase will be altered, as shown in figure 3. For comparison, in the inset we also include the corresponding curve for $G0$, for which the geometric phase is missing, where the angle θ_2 is chosen as $\pi/6$ and $\pi/4$. This indicates that the differential conductance at $\theta_2 = \pi/4$ is smaller than that at $\theta_2 = \pi/6$. This can be understood by noting that the incident electrons that we considered are only those with spin up in the left ferromagnet, i.e., the incident electrons are assumed to be perfectly polarized. Thus, the polarized electrons tunnel easily into the right ferromagnet when the angle θ_2 becomes smaller. $G0$ at $\theta_2 = \pi/6$ and $\pi/4$ increase with V_0 gradually; however, the differential conductance G becomes different when we consider the influence of the geometric phase. Each curve of the conductance G at $\theta_2 = \pi/4$ and $\pi/6$ has a big dip around 0.35 eV, whose value also becomes smaller than the differential conductance $G0$ in the absence of the geometric phase. This is due to the non-vanishing gradient term of the geometric phase in the expression for the probability flux density (23).

In figure 4, the differential conductance G associated with the geometric phase is compared for different magnitudes of the molecular fields h_1 and h_2 in the left and right

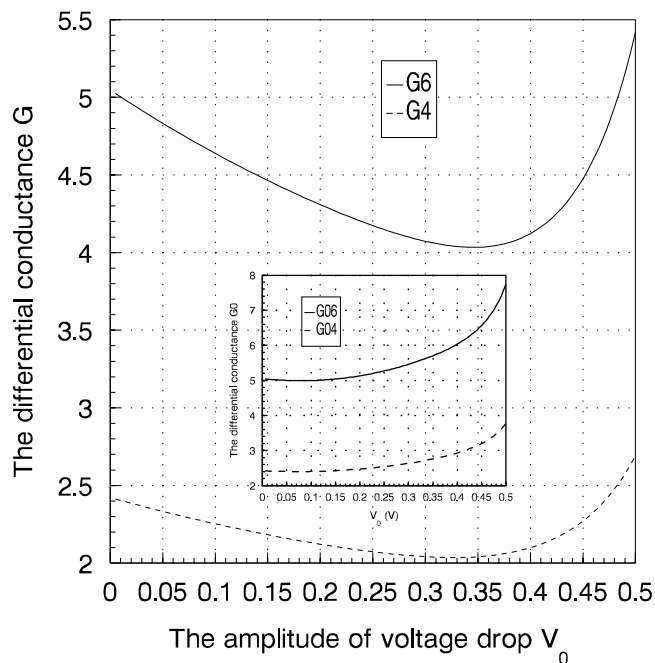


Figure 3. The conductance G (unit e^2/h) associated with the geometric phase versus V_0 at different angles of the molecular field, where the length of the insulator is 5 nm and the magnitudes of the molecular fields in the left and right ferromagnets are both 0.3 eV. The dashed curve shows the conductance G at $\theta_2 = \pi/4$ (denoted as $G4$) and the solid curve shows the conductance G at $\theta_2 = \pi/6$ (denoted as $G6$). The inset shows the conductance $G0$, for which the geometric phase is missing, the dashed curve shows the conductance $G0$ at $\theta_2 = \pi/4$ (denoted as $G04$) and the solid curve shows the conductance $G0$ at $\theta_2 = \pi/6$ (denoted as $G06$).

ferromagnets. Such a comparison shows that the value of the conductance G increases when both the molecular fields h_1 and h_2 are changed from 0.3 to 0.1 eV. This illustrates that tunnelling becomes relatively easy if the molecular fields in the ferromagnets are smaller. The inset shows the conductance $G0$ corresponding to the molecular fields taken as 0.3 eV and 0.1 eV, respectively. We see that the differential conductance G becomes smaller under the influence of the geometric phase; the curves of G have dips, while $G0$ increases with V_0 gradually, where the orientation angles of the molecular fields are chosen as $\theta_1 = 0$ and $\theta_2 = \pi/4$.

Finally, we present the tunnelling magnetoresistance as a function of V_0 in figure 5, where we choose both molecular fields h_1 and h_2 to be 0.3 eV. For comparison, we also include the curve of TMR0 for which the geometric phase has dropped out. It is seen that the TMR is obviously affected by the geometric phase. The TMR associated with the geometric phase has a big dip around 0.45 eV, whose value is smaller than TMR0. The character of the TMR is dominated by the differential conductance at $\theta_2 = 0$ and π according to the definition (22). In the inset the corresponding TMR and TMR0 curves, where we change the magnitude of the molecular fields h_1 and h_2 from 0.3 to 0.1 eV, are included. It indicates that the molecular fields play an important role in determining the shape of the tunnelling magnetoresistance; meanwhile, the value of the TMR in the molecular field 0.3 eV is larger than the TMR in the molecular field 0.1 eV, because in a smaller molecular field, the spin-polarized tunnelling becomes relatively easy due to the spin dependent scattering of conduction electrons being weaker.

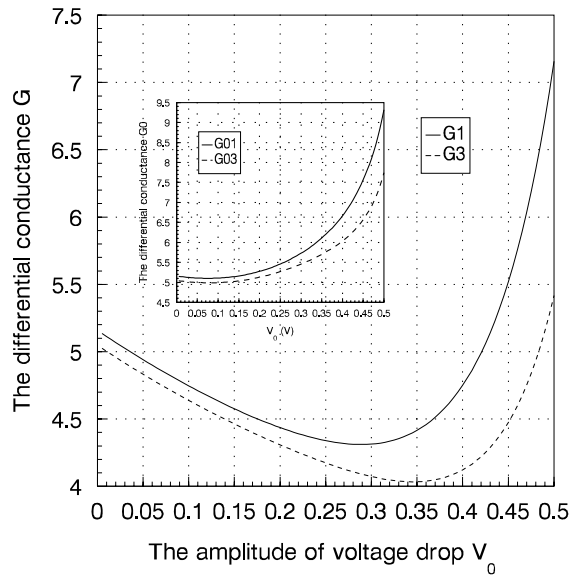


Figure 4. The conductance G (unit e^2/h) associated with the geometric phase versus V_0 at different magnitudes of the molecular field, where the length of the insulator is 5 nm and the angles θ_1 and θ_2 of the molecular fields in the left and right ferromagnets are 0 and $\pi/6$, respectively. The dashed curve shows the conductance G at $h_1 = h_2 = 0.3$ eV (denoted as $G3$) and the solid curve shows the conductance G at $h_1 = h_2 = 0.1$ eV (denoted as $G1$). The inset shows the conductance $G0$, for which the geometric phase is missing, the dashed curve shows the conductance $G0$ at $h_1 = h_2 = 0.3$ eV (denoted as $G03$) and the solid curve shows the conductance $G0$ at $h_1 = h_2 = 0.1$ eV (denoted as $G01$).

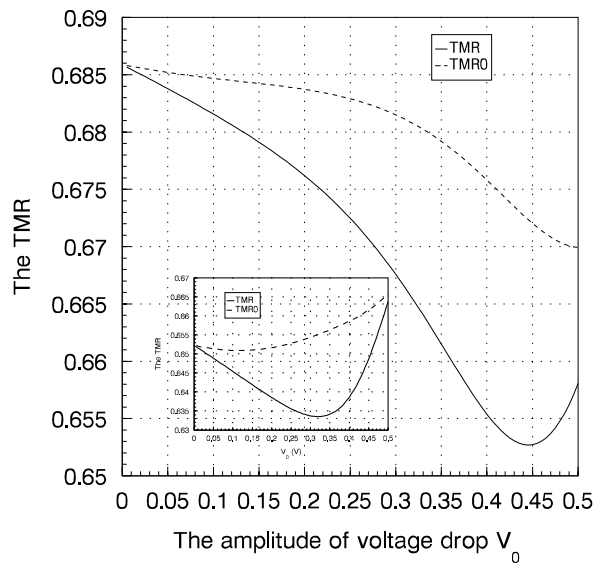


Figure 5. The TMR associated with the geometric phase and TMR0 for which the geometric phase is dropped out versus V_0 , where the length of the insulator is 5 nm, the magnitudes of both molecular fields in the left and right ferromagnets are 0.3 eV, the dashed line shows TMR0, the solid curve shows TMR under the influence of the geometric phase. The inset corresponds to the case of $h_1 = h_2 = 0.1$ eV, in which the dashed curve shows TMR0 and the solid line shows the TMR.

4. Summary and discussion

In this paper, we have studied the effect of the geometric phase on the spin-polarized tunnelling in a FM/I/FM junction. The effect is induced by the adiabatic variation of the time dependent voltage drop with time t applied to the insulator barrier. In order to demonstrate clearly the influence of the geometric phase on the physical quantities, we have numerically calculated the differential conductance and the tunnelling magnetoresistance as a function of the amplitude of the voltage drop, V_0 ; the results are presented in figures 2–5. The variations of the conductance and TMR with the angle θ_2 and the magnitude of the molecular field are also discussed. The comparison with the case in which the geometric phase is not considered indicates that the effect of the geometric phase on the spin-polarized tunnelling transport is obvious, and should not be ignored in the treatment. We have also suggested an experiment for confirming such an effect, induced by the geometric phase. However, we would like to point out that there exist simplifying assumptions in our model. First, the independent electron approximation is adopted, and the electron–electron interactions are not considered because they would make the equations hard to solve analytically. Second, the wavefunction in the insulator layer expressed in the semiclassical approximation is only up to first order, and the higher order effects are simply ignored for simplicity. Although our treatment has involved some assumptions as mentioned above, we believe that our result captures the primary characteristics of the effects induced by the geometric phase. How to extend our treatment to other complicated systems is an open question, which we leave to future work.

Acknowledgments

It is a pleasure to thank Dr Qing-Rong Zheng, Dr Biao Jin and Zheng-Gang Zhu for helpful discussions. This work was supported in part by the GSCAS president fund yzjj200102 and Ministry of Science And Technology Grant No 2002CCA02600.

Appendix

According to boundary conditions which require the continuity of the wavefunctions and their derivatives at the interfaces $x = 0$ and L , after some algebras, we can obtain the coefficients appearing in the wavefunctions as

$$C_{\uparrow} = \exp(-ik_{3\uparrow}d)(f_{11} * R_{\uparrow} + f_{12} * R_{\downarrow} + f_{13}), \quad (\text{A.1})$$

and

$$C_{\downarrow} = \exp(-ik_{3\downarrow}d)(f_{21} * R_{\uparrow} + f_{22} * R_{\downarrow} + f_{23}), \quad (\text{A.2})$$

where f_{1i} ($i = 1, 2, 3$) and f_{2i} ($i = 1, 2, 3$) take the following forms:

$$\begin{aligned} f_{1i} = & \cos(\theta_2) \exp(i\gamma^+(d, t)) [2m(E - V(d, t))]^{-\frac{1}{4}} \exp\left(\frac{i}{h} \int_0^d \sqrt{2m(E - V(x', t))} dx'\right) \\ & \times \frac{g_i}{(f_+ - f_-) \exp(i\gamma^+(0, t) - i\gamma^-(0, t))} + \cos(\theta_2) \\ & \times \exp(i\gamma^-(d, t)) [2m(E - V(d, t))]^{-\frac{1}{4}} \\ & \times \exp\left(-\frac{i}{h} \int_0^d \sqrt{2m(E - V(x', t))} dx'\right) h_i - \sin(\theta_2) \\ & \times \exp(i\gamma^+(d, t)) [2m(E - V(d, t))]^{-\frac{1}{4}} \end{aligned}$$

$$\begin{aligned}
& \times \exp\left(\frac{i}{h} \int_0^d \sqrt{2m(E - V(x', t))} dx'\right) \\
& \times \frac{k_i}{(f_+ - f_-) \exp(i\gamma^+(0, t) - i\gamma^-(0, t))} - \sin(\theta_2) \\
& \times \exp(i\gamma^-(d, t)) [2m(E - V(d, t))]^{-\frac{1}{4}} \\
& \times \exp\left(-\frac{i}{h} \int_0^d \sqrt{2m(E - V(x', t))} dx'\right) m_i, \tag{A.3}
\end{aligned}$$

and

$$\begin{aligned}
f_2 i &= \sin(\theta_2) \exp(i\gamma^+(d, t)) [2m(E - V(d, t))]^{-\frac{1}{4}} \exp\left(\frac{i}{h} \int_0^d \sqrt{2m(E - V(x', t))} dx'\right) \\
& \times \frac{g_i}{(f_+ - f_-) \exp(i\gamma^+(0, t) - i\gamma^-(0, t))} + \sin(\theta_2) \\
& \times \exp(i\gamma^-(d, t)) [2m(E - V(d, t))]^{-\frac{1}{4}} \\
& \times \exp\left(-\frac{i}{h} \int_0^d \sqrt{2m(E - V(x', t))} dx'\right) h_i + \cos(\theta_2) \\
& \times \exp(i\gamma^+(d, t)) [2m(E - V(d, t))]^{-\frac{1}{4}} \\
& \times \exp\left(\frac{i}{h} \int_0^d \sqrt{2m(E - V(x', t))} dx'\right) \\
& \times \frac{k_i}{(f_+ - f_-) \exp(i\gamma^+(0, t) - i\gamma^-(0, t))} + \cos(\theta_2) \\
& \times \exp(i\gamma^-(d, t)) [2m(E - V(d, t))]^{-\frac{1}{4}} \\
& \times \exp\left(-\frac{i}{h} \int_0^d \sqrt{2m(E - V(x', t))} dx'\right) m_i, \tag{A.4}
\end{aligned}$$

with

$$\begin{aligned}
f_{\pm} &= i\gamma^{\pm}(0, t) \exp(i\gamma^{\pm}(0, t)) [2m(E - V(0, t))]^{-\frac{1}{4}} + \frac{m}{2} \exp(i\gamma^{\pm}(0, t)) \\
& \times [2m(E - V(0, t))]^{-\frac{5}{4}} V'(0, t) \pm \frac{i}{h} \exp(i\gamma^{\pm}(0, t)) [2m(E - V(0, t))]^{\frac{1}{4}}, \tag{A.5}
\end{aligned}$$

and

$$g_1 = -i \cos(\theta_1) k_{1\uparrow} - f_- \exp(-i\gamma^-(0, t)) [2m(E - V(0, t))]^{\frac{1}{4}} \cos(\theta_1), \tag{A.6}$$

$$g_2 = i \sin(\theta_1) k_{1\downarrow} - f_- \exp(-i\gamma^-(0, t)) [2m(E - V(0, t))]^{\frac{1}{4}} \sin(\theta_1), \tag{A.7}$$

$$g_3 = i \cos(\theta_1) k_{1\uparrow} - f_- \exp(-i\gamma^-(0, t)) [2m(E - V(0, t))]^{\frac{1}{4}} \cos(\theta_1), \tag{A.8}$$

$$h_1 = \cos(\theta_1) \exp(-i\gamma^-(0, t)) [2m(E - V(0, t))]^{\frac{1}{4}} - \frac{g_1}{f_+ - f_-}, \tag{A.9}$$

$$h_2 = -\sin(\theta_1) \exp(-i\gamma^-(0, t)) [2m(E - V(0, t))]^{\frac{1}{4}} - \frac{g_2}{f_+ - f_-}, \tag{A.10}$$

$$h_3 = \cos(\theta_1) \exp(-i\gamma^-(0, t)) [2m(E - V(0, t))]^{\frac{1}{4}} - \frac{g_3}{f_+ - f_-}, \tag{A.11}$$

$$k_1 = -i \sin(\theta_1) k_{1\uparrow} - f_- \exp(-i\gamma^-(0, t)) [2m(E - V(0, t))]^{\frac{1}{4}}, \tag{A.12}$$

$$k_2 = -i \cos(\theta_1) k_{1\downarrow} - f_- \exp(-i\gamma^-(0, t)) [2m(E - V(0, t))]^{\frac{1}{4}}, \tag{A.13}$$

$$k_3 = i \sin(\theta_1) k_{1\uparrow} - f_- \exp(-i\gamma^-(0, t)) [2m(E - V(0, t))]^{\frac{1}{4}}, \quad (\text{A.14})$$

$$m_1 = \sin(\theta_1) \exp(-i\gamma^-(0, t)) [2m(E - V(0, t))]^{\frac{1}{4}} - \frac{k_1}{f_+ - f_-}, \quad (\text{A.15})$$

$$m_2 = \cos(\theta_1) \exp(-i\gamma^-(0, t)) [2m(E - V(0, t))]^{\frac{1}{4}} - \frac{k_2}{f_+ - f_-}, \quad (\text{A.16})$$

$$m_3 = \sin(\theta_1) \exp(-i\gamma^-(0, t)) [2m(E - V(0, t))]^{\frac{1}{4}} - \frac{k_3}{f_+ - f_-}. \quad (\text{A.17})$$

Meanwhile,

$$R_{\uparrow} = \frac{(f_{13} - \frac{f_{33}}{ik_{3\uparrow}}) - R_{\downarrow}(f_{12} - \frac{f_{32}}{ik_{3\uparrow}})}{(f_{11} - \frac{f_{31}}{ik_{3\uparrow}})}, \quad (\text{A.18})$$

$$R_{\downarrow} = \frac{\left(\frac{f_{43}}{ik_{3\downarrow}} - f_{23} \right) - \left(\frac{(f_{13} - \frac{f_{43}}{ik_{3\uparrow}})(f_{21} - \frac{f_{41}}{ik_{3\downarrow}})}{(f_{11} - \frac{f_{31}}{ik_{3\uparrow}})} \right)}{\left((f_{22} - \frac{f_{42}}{ik_{3\downarrow}}) - \frac{(f_{21} - \frac{f_{41}}{ik_{3\downarrow}})(f_{12} - \frac{f_{32}}{ik_{3\uparrow}})}{(f_{11} - \frac{f_{31}}{ik_{3\uparrow}})} \right)}, \quad (\text{A.19})$$

where $f3i$ ($i = 1, 2, 3$) and $f4i$ ($i = 1, 2, 3$) are expressed as

$$f3i = g_+ \cos(\theta_2) \frac{g_i}{(f_+ - f_-) \exp(i\gamma^+(0, t) - i\gamma^-(0, t))} + g_- \cos(\theta_2) h_i \\ - g_+ \sin(\theta_2) \frac{k_i}{(f_+ - f_-) \exp(i\gamma^+(0, t) - i\gamma^-(0, t))} - g_- \sin(\theta_2) m_i, \quad (\text{A.20})$$

$$f4i = g_+ \sin(\theta_2) \frac{g_i}{(f_+ - f_-) \exp(i\gamma^+(0, t) - i\gamma^-(0, t))} + g_- \sin(\theta_2) h_i \\ + g_+ \cos(\theta_2) \frac{k_i}{(f_+ - f_-) \exp(i\gamma^+(0, t) - i\gamma^-(0, t))} + g_- \cos(\theta_2) m_i, \quad (\text{A.21})$$

with

$$g_{\pm} = i\gamma^{\pm}(d, t) \exp(i\gamma^{\pm}(d, t)) [2m(E - V(d, t))]^{-\frac{1}{4}} \exp\left(\pm \frac{i}{\hbar} \int_0^d \sqrt{2m(E - V(x', t))} dx'\right) \\ + \frac{m}{2} \exp(i\gamma^{\pm}(d, t)) [2m(E - V(d, t))]^{-\frac{5}{4}} V'(d, t) \\ \times \exp\left(\pm \frac{i}{\hbar} \int_0^d \sqrt{2m(E - V(x', t))} dx'\right) \\ - \frac{i}{\hbar} \exp(i\gamma^{\pm}(d, t)) [2m(E - V(d, t))]^{\frac{1}{4}} \\ \times \exp\left(\pm \frac{i}{\hbar} \int_0^d \sqrt{2m(E - V(x', t))} dx'\right). \quad (\text{A.22})$$

We have now obtained all coefficients needed in the expressions for the differential conductance and TMR.

References

- [1] Moodera J S, Kinder L R, Wong T M and Meservey R 1995 *Phys. Rev. Lett.* **74** 3273
- [2] Moodera J S and Kinder L R 1996 *J. Appl. Phys.* **79** 4724
- [3] Miyazaki T and Tezuka N 1995 *J. Magn. Magn. Mater.* **139** 1231
- [4] Tezuka N and Miyazaki T 1996 *J. Appl. Phys.* **79** 6262

- [5] Slonczewski J C 1989 *Phys. Rev. B* **39** 6995
- [6] Zhang X D, Li B Z, Sun G and Pu F C 1997 *Phys. Rev. B* **56** 5484
- [7] Li Y, Li B Z, Zhang W S and Dai D S 1998 *Phys. Rev. B* **57** 1079
- [8] For a recent review, see Jauho A P 1999 *Preprint* cond-mat/9911282
- [9] Büttiker M 1993 *J. Phys.: Condens. Matter* **5** 9361
Büttiker M 1999 *Preprint* cond-mat/9909126
- [10] Christen T and Büttiker M 1996 *Europhys. Lett.* **53** 523
- [11] Christen T and Büttiker M 1996 *Phys. Rev. Lett.* **77** 143
- [12] Wang Z C, Su G and Zheng Q R 2001 *Phys. Rev. B* **64** 014407
- [13] Messiah A 1962 *Quantum Mechanics* vol 2 (Amsterdam: North-Holland)
- [14] Berry M V 1984 *Proc. R. Soc. A* **392** 45
- [15] Thouless D J, Kohmoto M, Nightingale M P and Den Nijs M 1982 *Phys. Rev. Lett.* **49** 405
- [16] Thouless D J 1983 *Phys. Rev. B* **27** 6083
- [17] Brouwer P W 1998 *Phys. Rev. B* **58** R10135
- [18] Büttiker M, Thomas H and Prêtre A 1994 *Z. Phys. B* **94** 133
- [19] Avron J E, Algart A, Graf G M and Sadun L 2000 *Preprint* cond-mat/0002194
- [20] Zhou H-Q, Lundin U, Cho S Y and McKenzie R H 2004 *Phys. Rev. B* **69** 113308
- [21] Usmani O, Lutz E and Büttiker M 2002 *Phys. Rev. E* **66** 021111
- [22] Datta S 1995 *Electronic Transport in Mesoscopic System* (New York: Cambridge University Press)